Preliminary Data on the Measurement of the $\mu^+ - \beta^+$ Decay Spectrum*

K. M. CROWE, R. H. HELM, AND G. W. TAUTFEST
High-Energy Physics Laboratory, Stanford University, Stanford, California

(Received April 14, 1955)

The results of a preliminary nature on the $\mu-\beta$ decay spectrum are given. The data are consistent with a theory as proposed by Michel with a parameter $\rho=0.50\pm0.10$. The background and systematic errors are discussed.

HISTORICAL INTRODUCTION

THE experimental data[1–11] on the decay of the μ meson are confusing at present. Michel[12] has analyzed these spectra in terms of a generalized β decay where he has shown that for energies above a few Mev there is only a single-parameter family of theoretical spectra if the interaction representation obeys simple invariance requirements. The data have been analyzed[13] in terms of this parameter ρ, which can go from 0 to 1. The decay is assumed to go via two neutrinos,

$$\mu^+ \rightarrow \beta^+ + \nu + \nu,$$

in which case

$$N(E)dE \propto \frac{4E^2}{W^4}\left[3(W-E)+2\rho\left(\frac{4}{3}E-W\right)\right]dE, \quad (1)$$

where E is the energy of the positron and W is the upper-energy cutoff; $W=52.71\pm0.07$ Mev.[14,15] The present status is shown in Table I.

TABLE I. Summary of data on $\mu^+-\beta^+$ decay spectrum.

	ρ value	Method	Experimenter	Reference
1	0.23[a]	Spiral orbit spectrometer	Sagane, Gardner, Hubbard	2
2	0.41 ± 0.13	Photographic emulsions	Bramson and Havens	3
3	0.43 ± 0.15 (150 events)[a]	Cloud chamber	Lagarrique	5
4	0.26 ± 0.26	Cloud chamber	Hubbard	6
5	0.50 ± 0.13	Cloud chamber	Vilain and Williams	7
6	$0.23^{+0.03}_{-0.05}$	Spiral orbit spectrometer	Sagane, Dudziak, Vedder	8
7	...	Cloud chamber	Harrison *et al.*	9
8	0.6 ± 0.10	Cloud chamber ($\mu^-\rightarrow\beta^-$)	Lederman and Sargent	10
9	0.72 (42 events)	Photographic emulsions	Mabboux-Stromberg	11

[a] Using new value of muon mass ($W=52.7$).

In view of the interest in the analysis of the β decay of the muon, we present a brief account of an experiment in progress and give our preliminary β spectrum.

APPARATUS AND PROCEDURE

Figures 1 and 2 show the experimental apparatus. The analyzed and collimated electron beam of approximately 400 Mev is from the Stanford Mark III linear electron accelerator. The beam is $\frac{3}{8}$ to $\frac{1}{2}$ in. in diameter; beam current is 5×10^9 electrons per pulse measured by a secondary-emission monitor.[16] The beam strikes a lead radiator 0.065-in. thick; the x-radiation and electrons pass through a target of lithium 1-in.$\times$1-in.$\times$2-in. long. Low-energy mesons produced in the lithium come to rest with relatively uniform density in the target. The positive pions decay to muons, which also stop and decay into positrons with the characteristic 2.2-μsec mean life. The positrons which leave the target at 90° to the beam enter the vacuum chamber of a double-focusing magnetic spectrometer.[17]

After magnetic analysis, the positrons are detected by making a fast coincidence between two $\frac{1}{8}$-in. thick scintillation counters, $1\frac{7}{8}$ in. by $1\frac{1}{2}$ in., spaced two inches apart, with time resolution 5×10^{-8} sec. This output is then placed into a delayed-coincidence gear

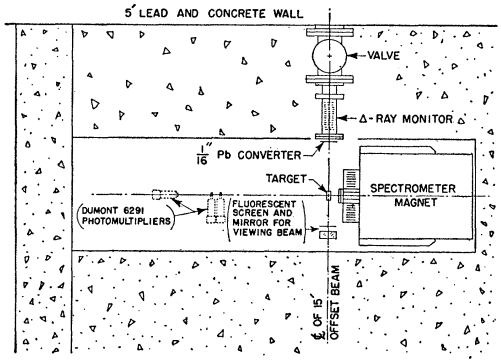

FIG. 1. Top view of experimental arrangement.

* The research reported here was supported by the joint program of the Office of Naval Research and the U. S. Atomic Energy Commission.

[1] Leighton, Anderson, and Seriff, Phys. Rev. **75**, 1432 (1949).
[2] Sagane, Gardner, and Hubbard, Phys. Rev. **82**, 557 (1951).
[3] H. Bramson and W. Havens, Phys. Rev. **83**, 861 (1951); **88**, 304 (1952).
[4] A. Lagarrique and C. Peyrou, J. phys. radium **12**, 848 (1951).
[5] A. Lagarrique, Compt. rend. **234**, 2060 (1952); and private communication.
[6] H. Hubbard, University of California Radiation Laboratory Report No. 1623 (unpublished).
[7] J. H. Vilain and R. W. Williams, Phys. Rev. **92**, 1586 (1953); **94**, 1011 (1954).
[8] Sagane, Dudziak, and Vedder, Phys. Rev. **95**, 863 (1954).
[9] Harrison, Cowan, and Reins, Nucleonics **12**, No. 3, 44 (1954).
[10] L. M. Lederman and C. R. Sargent (private communication to R. Sagane).
[11] C. Mabboux-Stromberg, Ann. phys. **9**, 441 (1954).
[12] L. Michel, Proc. Phys. Soc. (London) **A63**, 514 (1950).
[13] H. J. Bramson, Phys. Rev. **98**, 1187(A) (1955).
[14] Birnbaum, Smith, and Barkas, Phys. Rev. **91**, 765 (1953).
[15] K. M. Crowe and R. H. Phillips, Phys. Rev. **96**, 470 (1954).
[16] G. W. Tautfest and H. R. Fechter, Rev. Sci. Instr. **26**, 229 (1955).
[17] Snyder, Rubin, Fowler, and Lauritsen, Rev. Sci. Instr. **21**, 852 (1950).

which allows counting after the beam pulse. This equipment was built for pion-production experiments[18] by C. Newton, W. S. C. Williams, J. A. Narud, G. Masek, and W. K. H. Panofsky. The gates where counts are recorded are arranged as follows: Gate No. I opens 2.2 μsec after the beam pulse and remains open for 2.2 μsec; gate No. II opens 4.4 μsec after the beam pulse and remains open for 4.4 μsec.

Figure 3 shows the spectrum obtained by varying the current in the spectrometer magnet windings. The maximum magnetic field is approximately 4500 gauss. The curves plotted are the folds of our resolution into various theoretical spectra. The normalization of the folded theoretical curves to the data is arbitrary.

The resolving power of the system is made up of two major parts: (1) The energy loss of the positrons leaving the target; and (2) the finite heights of the target source and the detector crystal. (The shapes of these resolutions are shown in Fig. 4.)

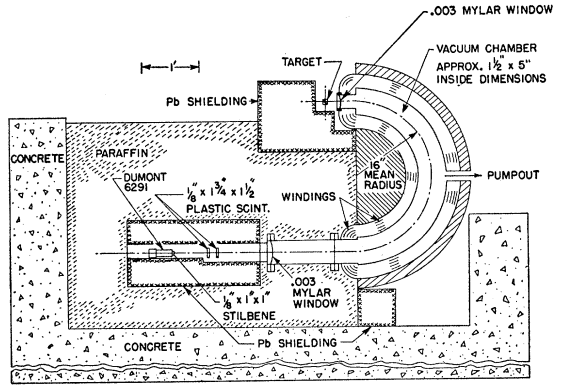

FIG. 2. Side view showing magnet section and counter location.

ANALYSIS OF DATA

The data as shown in Fig. 3 have been corrected for background and the variation in efficiency arising from the constant momentum resolution of the spectrometer. This causes a yield proportional to E times the spectrum which gives approximately an E^3 variation for the yield from Eq. (1). This imposes extremely low background conditions on the study of the low-energy portion of the spectrum.

Our background is of two types: (1) Pions of low energy also leave the target, pass through the spectrometer, and can stop in the first or second counter, depending on their range. These decay and some of the positrons will cause real coincidences with the proper period, the number depending on the solid angle of one counter relative to the other. We have varied this solid angle by a factor of ten by substituting a 1-in.×1-in. ×⅛-in. counter six inches behind the original second counter as indicated in Fig. 2. Results are shown in Fig. 5. There is no discernible change within rather poor

[18] Panofsky, Newton, and Yodh, Phys. Rev. **98**, 751 (1955).

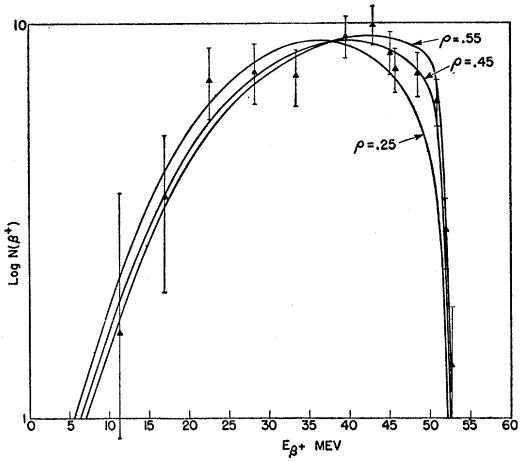

FIG. 3. Data on μ decay obtained with 1-in. by 1-in. lithium target 2-in. long in primary beam direction. Solid curves are obtained by folding the theoretical spectra into our resolution. The vertical normalization of the data to the curves is arbitrary.

statistics in the region of the end point and we believe this effect to be negligible in either geometry. The pions that stop in other places will also produce a real signal indistinguishable from the assumed process. This also is checked by substituting a carbon target which will have a larger real signal relative to those events compared to lithium because of the larger stopping power of carbon. We observe no significant change in the data in the low-energy region.

(2) The second type of delayed background is extremely puzzling. There is a background of neutron-

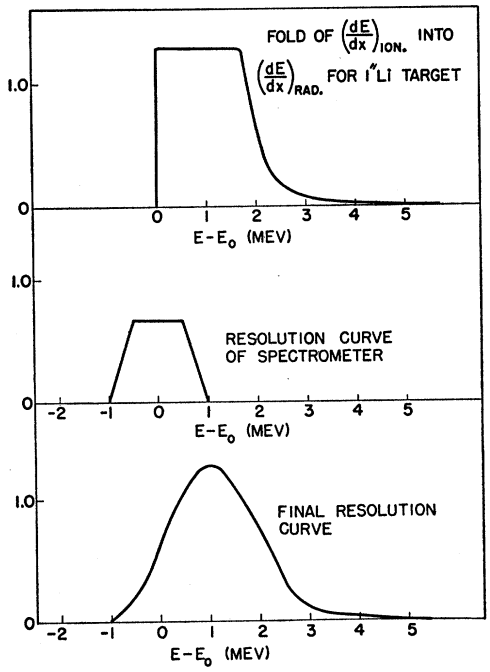

FIG. 4. Resolution curves for 1-in. lithium target.

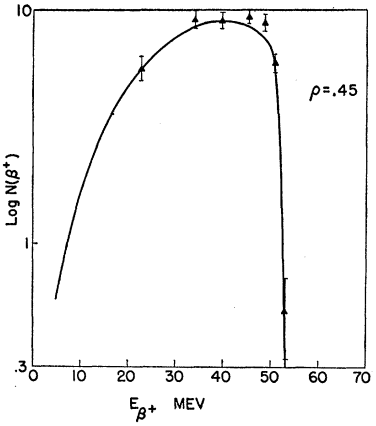

FIG. 5. Lithium data with (improved) counter geometry, without correction for long-period background.

induced counts which is present with no field; this appears to be small. At low-energy settings we find our counts are several times larger than the real signal and we notice that the decay period is not that of the real signal. These events are real coincidences from the lithium target, and they vary slowly with field and do not occur for reversed polarity. In the figures we have used the decay-period information to subtract off the false counts due to any effect with a long decay period (of the order of or greater than 40 μsec). Table II shows the treatment of the data assuming that the background has a period $\tau_B=20\tau_\beta$. Then, if S_β and B are the magnitudes of the μ-decay signal and the background, respectively, and $C_{\rm I}$ and $C_{\rm II}$ are the counts in the two delayed gates, we have

$$C_{\rm I}=S_\beta\int_0^{t_{\rm I}} e^{-t/\tau_\beta}\,dt+B\int_0^{t_{\rm I}} e^{-t/\tau_B}\,dt, \qquad (2)$$

$$C_{\rm II}=S_\beta\int_{t_{\rm I}}^{t_{\rm II}} e^{-t/\tau_\beta}\,dt+B\int_{t_{\rm I}}^{t_{\rm II}} e^{-t/\tau_B}\,dt. \qquad (3)$$

Above 30 Mev, the entire background is small and does not vary with field within statistics. Although the status of the low-energy points is unsatisfactory, the evaluation of the data does not necessarily involve these points and the detector system (with additional 6-in. spacing between counters) used to check the other real pion effect does not show an appreciable amount of the long-period background. This is evident in Fig. 5, where we have plotted the sum of the counts in the two gates without correction for long-period background (we have subtracted out the target-out counts).

We conclude, therefore, that with better detector geometry the effect may disappear altogether, and that making the subtraction described above is the better (although poor) alternative to getting a better detection geometry. Unfortunately, an accident in the form of an electrical fire made necessary the complete rewinding of the spectrometer magnet. Consequently, it will not be possible to obtain any further experimental data for several months from this writing.

RESULTS

The data show a very sharp upper end resolved to four percent at half-maximum. The end point at present is calibrated only very crudely (approximately two-percent error).

We conclude from the data that the spectrum obtained is consistent with a β-coupling characterized by a 'Michel' parameter of $\rho=0.50\pm0.07$, where the error is based upon statistics alone. Combining the systematic errors of about the same size we obtain $\rho=0.50\pm0.10$.

TABLE II. Correction to data for long-period background. Columns $C_{\rm I}$ and $C_{\rm II}$ are the counts in the two delayed gates; S_β and B are the signal and background computed using Eqs. (2) and (3), with $t_{\rm I}=\tau_\beta$ and $t_{\rm II}=2.4\tau_\beta$.

E (Mev)	$C_{\rm I}$	$C_{\rm II}$	S_β	B
7.9	32	47	−9.5	38.7
11.3	50	56	16.9	40.0
17.0	71	61	57.8	35.1
22.6	123	78	150.6	28.3
28.3	153	91	198.1	28.1
33.9	181	109	232.2	34.9
39.6	232	116	340.7	16.7
43.0	267	132	394.8	17.5
45.2	266	155	350.6	45.2
46.3	242	137	326.2	36.4
48.6	242	133	333.6	31.8
50.9	216	119	297.2	28.6
52.0	112	67	144.2	21.0
52.6	66	50	66.0	24.7
53.7	25	19	24.9	9.5

We find it entirely impossible to devise any mechanism to change our resolution or efficiency or background in the region of most significance (40–50 Mev) to alter these conclusions significantly. However, we must admit that the same remark applies to most of the other experiments with which we do not agree. In particular, the latest result of Sagane *et al.*[8] seems to be extremely accurate and the result entirely different. We are grateful to Dr. Sagane for informing us of his progress and for suggesting many checks which we hope to perform in the future.

ACKNOWLEDGMENTS

We should like to thank all those who contributed to the attainment of the high current density of the external beam of the Mark III linear accelerator.